Acta Cryst E CRYSTALLOGRAPHIC COMMUNICATIONS

ISSN 2056-9890

Synthesis, crystal structure and Hirshfeld surface analysis of 3,3′-[ethane-1,2-diylbis(sulfanediyl)]-bis(1*H*-1,2,4-triazol-5-amine)

Shakhnoza Mavlonova,[a] Giyosiddin Khayrullaev,[a] Dilnoza Rakhmonova,[a] Mirigul Berdimuratova,[b] Shakhnoza Kadirova,[a] Jamshid Ashurov[c] and Batirbay Torambetov[a]*

[a]National University of Uzbekistan named after Mirzo Ulugbek, 4 University St., Tashkent, 100174, Uzbekistan, [b]Karakalpak State University, 1 Ch. Abdirov St. Nukus, 230112, Uzbekistan, and [c]Institute of Bioorganic Chemistry, Academy of Sciences of Uzbekistan, M. Ulugbek St., 83, Tashkent, 100125, Uzbekistan. *Correspondence e-mail: torambetov_b@mail.ru

Received 23 March 2026
Accepted 2 April 2026

Edited by B. Therrien, University of Neuchâtel, Switzerland

Keywords: molecular structure; crystal structure; 1,2,4-triazole; hydrogen bond; Hirshfeld analysis.

CCDC reference: 2543358

Supporting information: this article has supporting information at journals.iucr.org/e

The title compound, $C_6H_{10}N_8S_2$, crystallizes in the monoclinic crystal system with $P2_1/c$ space group. The molecular geometry features a flexible ethylenedithio spacer inducing a 76.69 (11)° dihedral angle between triazole moieties; this twist precludes π–π stacking. The crystal cohesion is instead driven by a two-dimensional supramolecular framework maintained by strong N—H···N hydrogen bonds and auxiliary N···S and C···S contacts. Quantitative Hirshfeld surface analysis confirms the dominance of hydrogen-involving interactions (98.8%), with N···H (40.4%) and H···H (27.1%) as the primary contributors to the packing arrangement.

1. Chemical context

The 1,2,4-triazole ring is an important five-membered heterocyclic scaffold containing three nitrogen atoms that impart distinctive electronic characteristics and a relatively high dipole moment (Kaur & Chawla, 2017; El–Sebaey, 2020; Naeem, *et al.*, 2025). It has attracted considerable interest in coordination chemistry, where the differing nucleophilicity enables diverse coordination modes, including monodentate, bidentate, and bridging arrangements (Zhang *et al.*, 2008; Deswal *et al.*, 2024; Bodurlar *et al.*, 2025; Bader *et al.*, 2020). Derivatives of 1,2,4-triazole are also well known for their wide range of biological activities, such as anticancer, antioxidant, analgesic, antimalarial, antituberculosis, insecticidal, antimycobacterial, antimicrobial, anticonvulsant, anti-inflammatory, antifungal, and antibacterial properties (El-Sherief *et al.*, 2018; Sathyanarayana & Poojary, 2020; Wen *et al.*, 2020; Gultekin *et al.*, 2018). Representative examples of triazole are reported by Nuralieva *et al.* (2025), Pirimova *et al.* (2022), and Torambetov *et al.* (2025). Such compounds function as multitopic ligands bearing both thiol (–SH) and amine ($–NH_2$) functional groups. The presence of this soft sulfur and hard nitrogen donor atoms allows these molecules to participate in a range of coordination environments, facilitating the formation of complex, high-dimensional crystalline architectures stabilized by extensive hydrogen-bonding networks in metal complexes (Lin *et al.*, 2017; Ma *et al.*, 2008; Rakova *et al.*, 2003). As a continuation of our previous work (Khayrullaev, *et al.*, 2023), we report here the synthesis and single-crystal structural characterization of 3,3′-[ethane-1,2-diylbis(sulfanediyl)]bis(1*H*-1,2,4-triazol-5-amine), a derivative containing

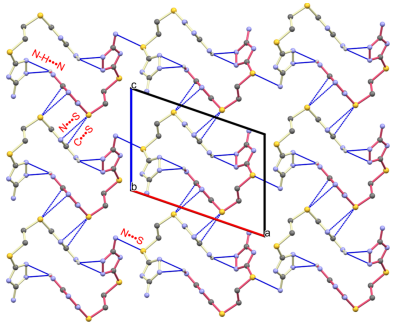

two (3-amino-1,2,4-triazol-5-yl)sulfanyl units interconnected through an ethylene spacer.

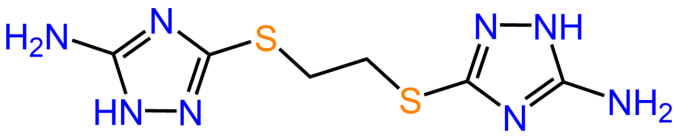

2. Structural commentary

The title compound crystallizes in the monoclinic system in the $P2_1/c$ (No. 14) space group with one molecule in the asymmetric unit (Fig. 1). The molecule consists of two (3-amino-1,2,4-triazol-5-yl)sulfanyl units bridged by an ethylene spacer. The molecular geometry is characterized by a pronounced non-coplanar orientation, with the two triazole moieties separated by a dihedral angle of 76.69 (11)° between their mean planes. This significant twist in the molecular backbone is attributed to the conformational flexibility of the ethylenedithio spacer. Consequently, this nearly orthogonal orientation prevents the triazole rings from achieving the facial alignment necessary for π–π stacking, shifting the burden of crystal consolidation onto the extensive hydrogen-bonding network.

3. Supramolecular features

The crystal packing is governed by a sophisticated network of non-covalent interactions rather than traditional stacking motifs. A view of the packing diagram along the *b*-axis reveals that adjacent 1D molecular chains are linked via N—H···N [N8–H8*A*···N1 = 2.62 (3) Å; Table 1] hydrogen bonds, which facilitate the assembly of molecular units along the *a*-axis direction (Fig. 2). Beyond the primary hydrogen-bonding interactions, the structural architecture is further reinforced by auxiliary N···S [3.361 (2) Å] and C···S [3.525 (2) Å] intermolecular contacts. Although these interactions are weaker than N—H···N interactions, the heteroatom contacts collectively bridge the molecular layers, consolidating the 2D supramolecular framework. The 76.69 (11)° dihedral twist previously mentioned precludes any π–π stacking, thereby increasing reliance on these specific hydrogen bonds and sulfur-mediated contacts for overall crystal cohesion.

Table 1
Hydrogen-bond geometry (Å, °).

D—H···*A*	*D*—H	H···*A*	*D*···*A*	*D*—H···*A*
N6—H6···N7^{i}	0.86	1.99	2.838 (2)	167
N2—H2···N5^{ii}	0.86	2.05	2.877 (2)	160
N8—H8*A*···N1^{iii}	0.76 (3)	2.62 (3)	3.232 (3)	140 (2)
N4—H4*A*···N1^{ii}	0.83 (3)	2.56 (3)	3.346 (3)	159 (2)
N8—H8*B*···S2^{i}	0.85 (3)	2.80 (3)	3.615 (2)	162 (3)
N4—H4*B*···N3^{iv}	0.90 (3)	2.13 (3)	3.010 (3)	168 (3)

Symmetry codes: (i) $-x+1, y-\frac{1}{2}, -z+\frac{3}{2}$; (ii) $x, -y+\frac{1}{2}, z-\frac{1}{2}$; (iii) $-x+1, -y+1, -z+1$; (iv) $-x, -y+1, -z$.

4. Hirshfeld surface and fingerprint analysis

Hirshfeld surface (HS) analysis (Spackman & Jayatilaka, 2009) and two-dimensional fingerprint plots (Spackman & McKinnon, 2002) were performed using *CrystalExplorer* (Spackman *et al.*, 2021). Quantitative Hirshfeld surface analysis demonstrates that the crystal packing is primarily consolidated by hydrogen-involving interactions, which account for a substantial 98.8% of the total surface area. The intermolecular contact distribution is dominated by N···H (40.4%), followed by H···H (27.1%), S···H (17.9%), C···H (5.1%), and minor contributions from C···S (4.1%) and N···S (4.1%). The Hirshfeld surface displays prominent dark-red spots, signifying close contacts that are significantly shorter than the sum of the van der Waals radii (Fig. 3). These spots

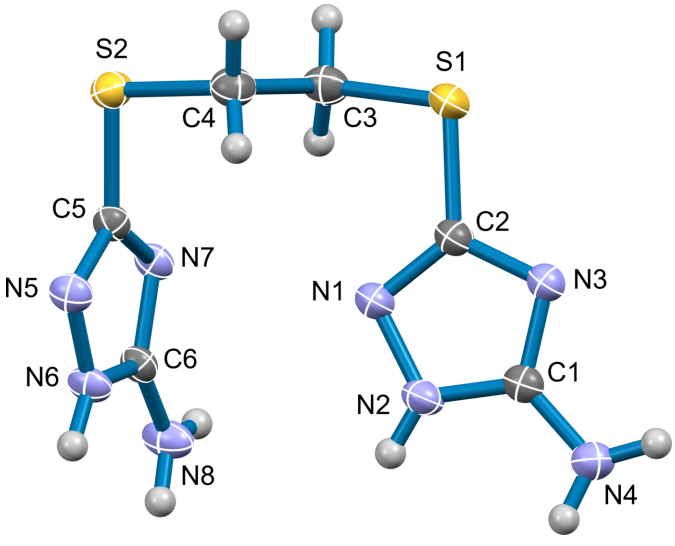

Figure 1
The title compound with displacement ellipsoids at the 50% probability level. For visual clarity, hydrogen atoms are represented as spheres of arbitrary size.

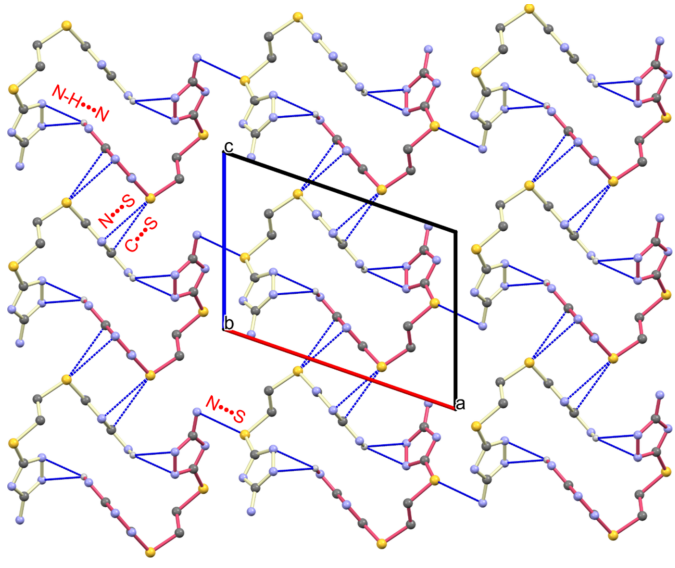

Figure 2
Packing arrangement viewed along the *b* axis, illustrating the network of intermolecular N—H···N, N···S, and C···S interactions.

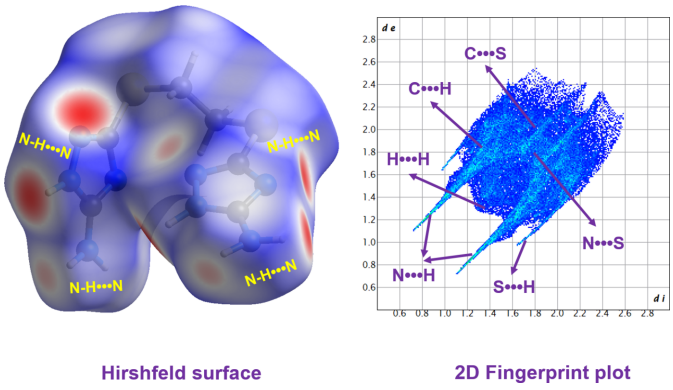

Figure 3
Hirshfeld surface and two-dimensional fingerprint plot.

are primarily attributed to strong N—H···N hydrogen bonding between adjacent molecular units. This is further corroborated by the 2D fingerprint plots, which reveal characteristic spikes for N···H interactions at approximately $d_i + d_e = 1.8$ Å and H···H contacts at $d_i + d_e = 2.6$ Å.

5. Database survey

A search of the Cambridge Structural Database (CSD) using the ConQuest program (Version 6.01, November 2025; Groom *et al.*, 2016) identified only 44 crystal structures containing the 3-amino-5-mercapto-1,2,4-triazole moiety. Of these, 25 are organic compounds and 19 are metal-based systems incorporating Fe, Co, Ni, Cu, Ag, Cd, Sn, Pr, Ho, Er, and Re. Among these structures, only two compounds contain two triazole moieties within the same molecule, in which the triazole units are linked by a disulfide bridge (DILZIL, Khayrullaev *et al.*, 2023; SEDMEV, Yang *et al.*, 2012). Notably, to date, no crystal structure has been reported featuring two (3-amino-1,2,4-triazol-5-yl)sulfanyl moieties linked by an ethylene spacer, underscoring the novelty of the present study.

6. Synthesis and crystallization

3-Amino-5-mercapto-1,2,4-triazole (1.16 g, 0.01 mol) and KOH (0.56 g, 0.01 mol) were dissolved in methanol (25 mL). The reaction mixture was cooled to 273 K, and 1,2-dichloroethane (0.005 mol) was added dropwise with stirring. The mixture was then refluxed at 338 K for 8 h. The reaction progress was monitored by thin-layer chromatography (TLC). After completion of the reaction, the solvent was removed under reduced pressure. The residue was dissolved in water (30 mL) and extracted with ethyl acetate (3 × 30 mL). The combined organic layers were dried over anhydrous Na_2SO_4, filtered, and concentrated under vacuum. The resulting solid was dried at room temperature for 4 days to afford colourless crystals (85% yield). The crude crystals was recrystallized from methanol solution.

Table 2
Experimental details.

Crystal data	
Chemical formula	$C_6H_{10}N_8S_2$
M_r	258.34
Crystal system, space group	Monoclinic, $P2_1/c$
Temperature (K)	293
a, b, c (Å)	12.7401 (2), 9.8361 (1), 9.2113 (2)
β (°)	109.069 (2)
V (Å^3)	1090.95 (3)
Z	4
Radiation type	Cu $K\alpha$
μ (mm^{-1})	4.35
Crystal size (mm)	0.18 × 0.12 × 0.1
Data collection	
Diffractometer	XtaLAB Synergy, Single source at home/near, HyPix3000
Absorption correction	Multi-scan (*CrysAlis PRO*; Rigaku OD, 2021)
T_{min}, T_{max}	0.615, 1.000
No. of measured, independent and observed [$I > 2\sigma(I)$] reflections	10263, 2107, 1927
R_{int}	0.031
(sin $\theta/\lambda)_{max}$ (Å^{-1})	0.614
Refinement	
$R[F^2 > 2\sigma(F^2)]$, $wR(F^2)$, S	0.035, 0.100, 1.09
No. of reflections	2107
No. of parameters	161
H-atom treatment	H atoms treated by a mixture of independent and constrained refinement
$\Delta\rho_{max}$, $\Delta\rho_{min}$ (e Å^{-3})	0.40, −0.24

Computer programs: *CrysAlis PRO* (Rigaku OD, 2021), *SHELXT2014/5* (Sheldrick, 2015*a*), *SHELXL2016/6* (Sheldrick, 2015*b*) and *OLEX2* (Dolomanov *et al.*, 2009).

7. Refinement

Crystal data, data collection and structure refinement details are summarized in Table 2. All hydrogen atoms were located from difference-Fourier maps and refined isotropically.

Acknowledgements

BT is grateful to the FAIRE programme provided by the Cambridge Crystallographic Data Centre (CCDC) for the opportunity to use the Cambridge Structural Database (CSD) and associated software.

References

Bader, A. T., Rasheed, N. A., Aljeboree, M. & Alkaiml, A. F. (2020). *J. Phys. Conf. Ser.* **1664**, 012100.
Bodurlar, Y., Ozturk, I. I., Grześkiewicz, A. M., Kubicki, M., Banti, C. N. & Hadjikakou, S. K. (2025). *Inorg. Chem. Commun.* **183**, 115915.
Deswal, Y., Asija, S., Tufail, A., Dubey, A., Deswal, L., Kumar, N. & Barwa, P. (2024). *J. Inorg. Organomet. Polym. Mater.* **34**, 144–160.
Dolomanov, O. V., Bourhis, L. J., Gildea, R. J., Howard, J. A. K. & Puschmann, H. (2009). *J. Appl. Cryst.* **42**, 339–341.
El–Sebaey, S. A. (2020). *ChemistrySelect* **5**, 11654-11680.
El-Sherief, H. A., Youssif, B. G., Bukhari, S. N. A., Abdel-Aziz, M. & Abdel-Rahman, H. M. (2018). *Bioorg. Chem.* **76**, 314–325.
Groom, C. R., Bruno, I. J., Lightfoot, M. P. & Ward, S. C. (2016). *Acta Cryst.* B**72**, 171–179.

Gultekin, E., Kolcuoglu, Y., Akdemir, A., Sirin, Y., Bektas, H. & Bekircan, O. (2018). *ChemistrySelect* **3**, 8813-8818.
Kaur, P. & Chawla, A. (2017). *Int. Res. J. Pharm.* **8**, 10–29.
Khayrullaev, G., Torambetov, B., Kadirova, S. & Vaksler, Y. (2023). *Z. Kristallogr. New Cryst. Struct.* **238**, 141–144.
Lin, S., Cui, Y. Z., Qiu, Q. M., Han, H. L., Li, Z. F., Liu, M., Xin, X. L. & Jin, Q. H. (2017). *Polyhedron* **134**, 319–329.
Ma, C., Li, Y., Han, Y. & Zhang, R. (2008). *Inorg. Chim. Acta* **361**, 380–386.
Naeem, N., Mughal, E. U., Sadiq, A., Othman, G. A. & Shakoor, B. (2025). *Arch. Pharm.* **358**, e70059.
Nuralieva, G., Alieva, M., Torambetov, B., Leslee, D. B. C., Senthilkumar, B., Kaur, S., Dabke, N. B., Vanka, K., Ashurov, J., Kadirova, S. & Gonnade, R. G. (2025). *J. Mol. Struct.* **1338**, 142274.
Pirimova, M., Torambetov, B., Kadirova, S., Ziyaev, A., Gonnade, R. G. & Ashurov, J. (2022). *Acta Cryst.* E**78**, 794–797.
Rakova, O. A., Sanina, N. A., Aldoshin, S. M., Goncharova, N. V., Shilov, G. V., Shulga, Y. M. & Ovanesyan, N. S. (2003). *Inorg. Chem. Commun.* **6**, 145–148.
Rigaku OD (2021). *CrysAlis PRO*. Rigaku Oxford Diffraction, Yarnton, England.
Sathyanarayana, R. & Poojary, B. (2020). *J. Chin. Chem. Soc.* **67**, 459–477.
Sheldrick, G. M. (2015*a*). *Acta Cryst.* A**71**, 3–8.
Sheldrick, G. M. (2015*b*). *Acta Cryst.* C**71**, 3–8.
Spackman, M. A. & Jayatilaka, D. (2009). *CrystEngComm* **11**, 19–32.
Spackman, M. A. & McKinnon, J. J. (2002). *CrystEngComm* **4**, 378–392.
Spackman, P. R., Turner, M. J., McKinnon, J. J., Wolff, S. K., Grimwood, D. J., Jayatilaka, D. & Spackman, M. A. (2021). *J. Appl. Cryst.* **54**, 1006–1011.
Torambetov, B., Khojabaeva, G., Bharty, M. K., Gupta, S. K., Kadirova, S., Pradeep, S., Dastager, S. G. & Gonnade, R. G. (2025). *J. Mol. Struct.* **1354**, 144763.
Wen, X., Zhou, Y., Zeng, J. & Liu, X. (2020). *Curr. Top. Med. Chem.* **20**, 1441–1460.
Yang, W., Qiu, Q.-M., Jin, Q.-H. & Zhang, C.-L. (2012). *Acta Cryst.* E**68**, o3194.
Zhang, R. B., Li, Z. J., Cheng, J. K., Qin, Y. Y., Zhang, J. & Yao, Y. G. (2008). *Cryst. Growth Des.* **8**, 2562–2573.

supporting information

Acta Cryst. (2026). E**82**, 446-449 [https://doi.org/10.1107/S2056989026003464]

Synthesis, crystal structure and Hirshfeld surface analysis of 3,3′-[ethane-1,2-diylbis(sulfanediyl)]bis(1*H*-1,2,4-triazol-5-amine)

Shakhnoza Mavlonova, Giyosiddin Khayrullaev, Dilnoza Rakhmonova, Mirigul Berdimuratova, Shakhnoza Kadirova, Jamshid Ashurov and Batirbay Torambetov

Computing details

3,3′-[Ethane-1,2-diylbis(sulfanediyl)]bis(1*H*-1,2,4-triazol-5-amine)

Crystal data

$C_6H_{10}N_8S_2$
$M_r = 258.34$
Monoclinic, $P2_1/c$
$a = 12.7401$ (2) Å
$b = 9.8361$ (1) Å
$c = 9.2113$ (2) Å
$\beta = 109.069$ (2)°
$V = 1090.95$ (3) Å^3
$Z = 4$
$F(000) = 536$
$D_x = 1.573$ Mg m^{-3}
Cu $K\alpha$ radiation, $\lambda = 1.54184$ Å
Cell parameters from 6441 reflections
$\theta = 3.7$–70.8°
$\mu = 4.35$ mm^{-1}
$T = 293$ K
Block, colourless
0.18 × 0.12 × 0.1 mm

Data collection

XtaLAB Synergy, Single source at home/near, HyPix3000 diffractometer
Radiation source: micro-focus sealed X-ray tube, PhotonJet (Cu) X-ray Source
Mirror monochromator
Detector resolution: 10.0000 pixels mm^{-1}
ω scans
Absorption correction: multi-scan (CrysAlisPro; Rigaku OD, 2021)
$T_{min} = 0.615$, $T_{max} = 1.000$
10263 measured reflections
2107 independent reflections
1927 reflections with $I > 2\sigma(I)$
$R_{int} = 0.031$
$\theta_{max} = 71.3°$, $\theta_{min} = 3.7°$
$h = -15\rightarrow15$
$k = -12\rightarrow11$
$l = -11\rightarrow11$

Refinement

Refinement on F^2
Least-squares matrix: full
$R[F^2 > 2\sigma(F^2)] = 0.035$
$wR(F^2) = 0.100$
$S = 1.09$
2107 reflections
161 parameters
0 restraints
Primary atom site location: dual
Hydrogen site location: mixed
H atoms treated by a mixture of independent and constrained refinement
$w = 1/[\sigma^2(F_o^2) + (0.0551P)^2 + 0.2828P]$ where $P = (F_o^2 + 2F_c^2)/3$
$(\Delta/\sigma)_{max} = 0.001$
$\Delta\rho_{max} = 0.40$ e Å^{-3}
$\Delta\rho_{min} = -0.24$ e Å^{-3}

Special details

Geometry. All esds (except the esd in the dihedral angle between two l.s. planes) are estimated using the full covariance matrix. The cell esds are taken into account individually in the estimation of esds in distances, angles and torsion angles; correlations between esds in cell parameters are only used when they are defined by crystal symmetry. An approximate (isotropic) treatment of cell esds is used for estimating esds involving l.s. planes.

Fractional atomic coordinates and isotropic or equivalent isotropic displacement parameters (Å²)

	x	*y*	*z*	U_{iso}*/U_{eq}
S2	0.31895 (4)	0.55253 (5)	0.90594 (6)	0.04855 (17)
S1	0.08980 (5)	0.65665 (5)	0.44295 (6)	0.05777 (19)
N7	0.47164 (12)	0.50710 (14)	0.75544 (17)	0.0401 (3)
N6	0.47018 (13)	0.28482 (15)	0.75254 (19)	0.0452 (4)
H6	0.485616	0.202665	0.734751	0.054*
N3	0.08227 (13)	0.50853 (16)	0.19660 (18)	0.0458 (4)
N5	0.39835 (13)	0.32119 (15)	0.82907 (19)	0.0459 (4)
N2	0.21243 (14)	0.35730 (16)	0.2911 (2)	0.0493 (4)
H2	0.255533	0.289118	0.295113	0.059*
N1	0.21245 (14)	0.43632 (17)	0.41680 (19)	0.0490 (4)
N8	0.58527 (17)	0.3923 (2)	0.6323 (3)	0.0594 (5)
N4	0.11720 (17)	0.3516 (2)	0.0219 (2)	0.0551 (4)
C5	0.40203 (14)	0.45463 (17)	0.8264 (2)	0.0390 (4)
C6	0.51240 (14)	0.39592 (17)	0.7099 (2)	0.0391 (4)
C1	0.13561 (15)	0.40294 (18)	0.1635 (2)	0.0435 (4)
C2	0.13288 (15)	0.52359 (19)	0.3502 (2)	0.0434 (4)
C4	0.19338 (17)	0.5601 (2)	0.7390 (2)	0.0521 (5)
H4C	0.178660	0.471254	0.691014	0.063*
H4D	0.130775	0.584750	0.771580	0.063*
C3	0.20554 (18)	0.6624 (2)	0.6248 (3)	0.0548 (5)
H3A	0.274469	0.645397	0.604546	0.066*
H3B	0.209829	0.752709	0.668612	0.066*
H8A	0.606 (2)	0.459 (3)	0.610 (3)	0.056 (7)*
H4A	0.147 (2)	0.276 (3)	0.022 (3)	0.061 (7)*
H8B	0.597 (2)	0.315 (3)	0.601 (3)	0.079 (9)*
H4B	0.058 (3)	0.384 (3)	−0.053 (3)	0.078 (9)*

Atomic displacement parameters (Å²)

	U^{11}	U^{22}	U^{33}	U^{12}	U^{13}	U^{23}
S2	0.0470 (3)	0.0517 (3)	0.0468 (3)	0.00188 (19)	0.0152 (2)	−0.00829 (19)
S1	0.0635 (3)	0.0539 (3)	0.0529 (3)	0.0241 (2)	0.0149 (2)	0.0000 (2)
N7	0.0423 (8)	0.0276 (7)	0.0507 (9)	−0.0013 (6)	0.0155 (7)	0.0015 (6)
N6	0.0512 (9)	0.0270 (7)	0.0612 (10)	0.0001 (6)	0.0238 (8)	−0.0008 (6)
N3	0.0443 (8)	0.0444 (8)	0.0483 (9)	0.0058 (7)	0.0145 (7)	0.0008 (7)
N5	0.0483 (8)	0.0344 (8)	0.0583 (10)	−0.0048 (6)	0.0220 (7)	−0.0004 (7)
N2	0.0513 (9)	0.0413 (8)	0.0576 (10)	0.0106 (7)	0.0209 (8)	0.0000 (7)
N1	0.0502 (9)	0.0451 (9)	0.0506 (9)	0.0114 (7)	0.0151 (7)	0.0003 (7)
N8	0.0710 (12)	0.0387 (10)	0.0846 (14)	0.0037 (9)	0.0474 (11)	0.0068 (9)

N4	0.0613 (11)	0.0509 (11)	0.0556 (11)	0.0043 (9)	0.0224 (9)	−0.0057 (8)
C5	0.0393 (9)	0.0329 (8)	0.0424 (9)	−0.0023 (7)	0.0101 (7)	−0.0020 (7)
C6	0.0405 (9)	0.0305 (8)	0.0453 (9)	−0.0007 (6)	0.0126 (7)	0.0018 (7)
C1	0.0421 (9)	0.0388 (9)	0.0532 (10)	−0.0026 (7)	0.0204 (8)	0.0012 (8)
C2	0.0414 (9)	0.0409 (9)	0.0492 (10)	0.0042 (7)	0.0164 (8)	0.0025 (8)
C4	0.0458 (10)	0.0536 (11)	0.0582 (12)	0.0014 (9)	0.0188 (9)	−0.0047 (9)
C3	0.0612 (12)	0.0431 (10)	0.0623 (13)	0.0015 (9)	0.0230 (10)	−0.0051 (9)

Geometric parameters (Å, º)

S2—C5	1.7580 (18)	N2—C1	1.338 (3)
S2—C4	1.822 (2)	N1—C2	1.317 (2)
S1—C2	1.7463 (19)	N8—C6	1.345 (3)
S1—C3	1.836 (2)	N8—H8A	0.76 (3)
N7—C5	1.363 (2)	N8—H8B	0.85 (3)
N7—C6	1.335 (2)	N4—C1	1.346 (3)
N6—H6	0.8600	N4—H4A	0.83 (3)
N6—N5	1.372 (2)	N4—H4B	0.90 (3)
N6—C6	1.332 (2)	C4—H4C	0.9700
N3—C1	1.330 (2)	C4—H4D	0.9700
N3—C2	1.358 (2)	C4—C3	1.500 (3)
N5—C5	1.314 (2)	C3—H3A	0.9700
N2—H2	0.8600	C3—H3B	0.9700
N2—N1	1.394 (2)		
C5—S2—C4	98.81 (9)	N7—C6—N8	126.52 (17)
C2—S1—C3	100.49 (9)	N6—C6—N7	110.08 (16)
C6—N7—C5	102.77 (14)	N6—C6—N8	123.40 (17)
N5—N6—H6	125.1	N3—C1—N2	110.01 (17)
C6—N6—H6	125.1	N3—C1—N4	125.09 (19)
C6—N6—N5	109.79 (14)	N2—C1—N4	124.88 (19)
C1—N3—C2	102.71 (15)	N3—C2—S1	118.24 (13)
C5—N5—N6	102.53 (14)	N1—C2—S1	125.31 (15)
N1—N2—H2	124.9	N1—C2—N3	116.44 (17)
C1—N2—H2	124.9	S2—C4—H4C	109.5
C1—N2—N1	110.14 (15)	S2—C4—H4D	109.5
C2—N1—N2	100.69 (16)	H4C—C4—H4D	108.1
C6—N8—H8A	119.0 (19)	C3—C4—S2	110.85 (15)
C6—N8—H8B	116 (2)	C3—C4—H4C	109.5
H8A—N8—H8B	124 (3)	C3—C4—H4D	109.5
C1—N4—H4A	113.2 (17)	S1—C3—H3A	109.1
C1—N4—H4B	116.8 (18)	S1—C3—H3B	109.1
H4A—N4—H4B	126 (2)	C4—C3—S1	112.54 (15)
N7—C5—S2	124.53 (13)	C4—C3—H3A	109.1
N5—C5—S2	120.63 (14)	C4—C3—H3B	109.1
N5—C5—N7	114.82 (16)	H3A—C3—H3B	107.8
S2—C4—C3—S1	171.73 (10)	C6—N7—C5—N5	0.7 (2)

N6—N5—C5—S2	177.82 (12)	C6—N6—N5—C5	0.3 (2)
N6—N5—C5—N7	−0.7 (2)	C1—N3—C2—S1	178.47 (14)
N5—N6—C6—N7	0.1 (2)	C1—N3—C2—N1	−0.6 (2)
N5—N6—C6—N8	−179.81 (18)	C1—N2—N1—C2	0.4 (2)
N2—N1—C2—S1	−178.83 (14)	C2—S1—C3—C4	−83.15 (16)
N2—N1—C2—N3	0.2 (2)	C2—N3—C1—N2	0.8 (2)
N1—N2—C1—N3	−0.7 (2)	C2—N3—C1—N4	−177.61 (18)
N1—N2—C1—N4	177.64 (18)	C4—S2—C5—N7	91.57 (16)
C5—S2—C4—C3	−77.89 (16)	C4—S2—C5—N5	−86.75 (16)
C5—N7—C6—N6	−0.48 (19)	C3—S1—C2—N3	−164.45 (15)
C5—N7—C6—N8	179.4 (2)	C3—S1—C2—N1	14.5 (2)
C6—N7—C5—S2	−177.68 (13)		

Hydrogen-bond geometry (Å, º)

D—H···*A*	*D*—H	H···*A*	*D*···*A*	*D*—H···*A*
N6—H6···N7^{i}	0.86	1.99	2.838 (2)	167
N2—H2···N5^{ii}	0.86	2.05	2.877 (2)	160
N8—H8*A*···N1^{iii}	0.76 (3)	2.62 (3)	3.232 (3)	140 (2)
N4—H4*A*···N1^{ii}	0.83 (3)	2.56 (3)	3.346 (3)	159 (2)
N8—H8*B*···S2^{i}	0.85 (3)	2.80 (3)	3.615 (2)	162 (3)
N4—H4*B*···N3^{iv}	0.90 (3)	2.13 (3)	3.010 (3)	168 (3)

Symmetry codes: (i) −*x*+1, *y*−1/2, −*z*+3/2; (ii) *x*, −*y*+1/2, *z*−1/2; (iii) −*x*+1, −*y*+1, −*z*+1; (iv) −*x*, −*y*+1, −*z*.